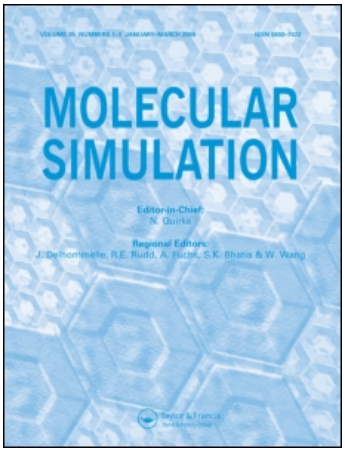

Molecular Simulation
Publication details, including instructions for authors and subscription information:
http://www.informaworld.com/smpp/title~content=t713644482

Application of the Free Energy Calculations to Study Drug-enzyme and Drug-dna Complexes

Piotr Cieplak[a]
[a] Department of Chemistry, University of Warsaw, Warsaw, Poland

Online publication date: 26 October 2010

To cite this Article Cieplak, Piotr(2002) 'Application of the Free Energy Calculations to Study Drug-enzyme and Drug-dna Complexes', Molecular Simulation, 28: 1, 173 — 186
To link to this Article: DOI: 10.1080/08927020211978
URL: http://dx.doi.org/10.1080/08927020211978

Molecular Simulation, 2002, Vol. 28(1–2), pp. 173–186

APPLICATION OF THE FREE ENERGY CALCULATIONS TO STUDY DRUG-ENZYME AND DRUG-DNA COMPLEXES

PIOTR CIEPLAK

Department of Chemistry, University of Warsaw, Pasteur 1, 02-093 Warsaw, Poland

(Received September 2000; accepted January 2001)

Applications of two free energy calculation approaches are presented to study drug-biomolecule complexes. The first method, the free energy perturbation (FEP) method and molecular dynamics simulations has been applied to study the JG-365 inhibitor bound to the HIV-aspartic protease. The FEP method has been applied to predict the consequence of replacing each of the seven peptide bonds in the JG-365 by trans-ethylene or fluoroethylene units. The necessary initial conformations of the inhibitor for "in water" perturbations have been found using neural network clustering approach applied to the long molecular dynamics trajectory of the inhibitor in water solution. The second method is applied to study binding free energies of some DNA-drug complexes and is based on analysis of long molecular dynamics trajectories by continuum solvent approach (MM/PBSA).

Keywords: Free energy perturbation; Continuum solvent; HIV; DNA-drug complexes

DRUG-ENZYME FREE ENERGY CALCULATIONS

Recently we applied the free energy perturbation method to study the consequence of replacing each of the seven peptide bonds by trans-ethylene or fluoroethylene units in the potent HIV aspartic protease inhibitor JG-365 [1–3]. HIV aspartic protease is one of the three, most important, proteins chosen as a main target for drug design in fighting AIDS disease [4, 5]. The two other targets are: the reverse transcriptase and integrase enzymes [6, 7].

The JG-365 is a hydroxyethylamine (HEA) analog of the ACE-SER-LEU-ASN-PHE-PRO-ILE-VAL-OMe peptide (Fig. 1) exhibiting 0.24 nM inhibition constant.

ISSN: 0892-7022 DOI: 10.1080/08927020290004449

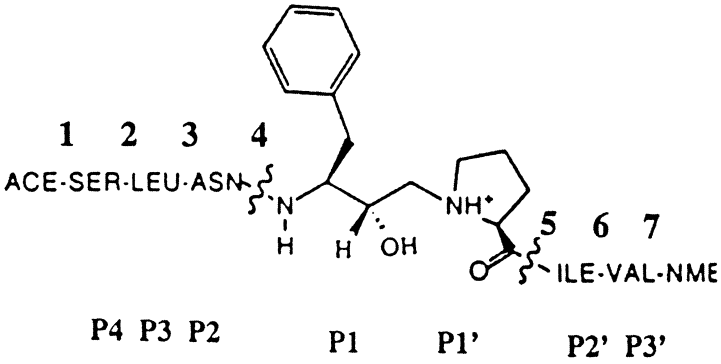

FIGURE 1 The structure of hydroxyethylamine analog of the JG-365 inhibitor.

The HEA modification of the peptide bond is located between PHE-PRO groups, mimicking the tetrahedral intermediate for hydrolysis of that peptide bond by the HIV protease. The proposed peptide bond modifications (by CH═CH and CF═CH groups) could be quite useful because of many reasons. They have geometry that is very similar to the original peptide bond, thus they do not change already appropriate conformation of the inhibitor needed in the active site, fulfilling appropriate conformational constraints. Olefin derivatives have lower polarity, and as such should facilitate passage through membranes and blood-brain barrier. The dipole magnitudes and orientations, as well as atomic charges of the CO—NH, CH═CH and CF═CH groups are presented in Figure 2.

Such pseudomimetics should exhibit increased resistance to the enzymatic degradation by amino-peptidase, maintaining longer duration of the modified inhibitor action. It was already demonstrated, that fluoro-olefin derivatives exhibited inhibitory effects on cyclophilin enzyme [8]. The olefin derivatives of enkephalins and substance P also exhibited bioactivity [9]. However, the main purpose of this study is not to advocate the usefulness of the modified JG-365 peptidomimetics in medicinal chemistry but to demonstrate one of the possible approaches, which could be helpful in the free energy calculations.

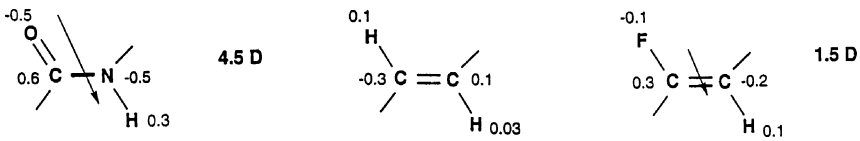

FIGURE 2 The dipole moments magnitude and orientation and atomic partial charges on —CO—NH—, —CH═CH— and —CF═CH— groups.

In our studies we applied the free energy perturbation approach [10, 11], which employs the following thermodynamic cycle (Fig. 3) in order to derive appropriate binding free energy differences between original compound and its chemical modification.

Since calculations of the horizontal processes cannot be easily performed, during free energy perturbation method, one alternatively simulates the two vertical processes in order to derive: $\Delta\Delta G_{bind} = \Delta G_{bind2} - \Delta G_{bind1} = \Delta G_{enz} - \Delta G_{solv}$. This approach involves calculations of the free energy differences between two inhibitors: Inh_2 and Inh_1 in aqueous solution (ΔG_{solv}) and in the enzymatic binding site (ΔG_{enz}). Those free energy differences are calculated during molecular dynamics simulations by perturbing one molecule (Inh_1) into another one (Inh_2) and collecting appropriate free energies calculated according to the following formula:

$$\Delta G = -RT \ln\langle \exp(-\Delta H/RT)_a \rangle, \quad (1)$$

where $\Delta H = H_b - H_a$, and the H_b and H_a are Hamiltonians for the states "b" (*e.g.*, Inh_2) and "a" (Inh_1), respectively, which can be represented by appropriate empirical force field parameters employed in the calculations.

All calculations pertaining to the G_{enz} values have been initiated from the inhibitor-enzyme crystallographic structure solved by Wlodawer *et al.* [12, 13]. In those cases calculated free energies were fairly well converged values, because of geometrical constraints the JG-365 inhibitor encounters in the active site. The protocol and results for the "in enzyme" simulations have been given in Ref. [1]. On the other hand calculations of the ΔG_{solv} is more complicated since JG365 is a flexible molecule and it is difficult to determine its representative conformations in aqueous solution, which should be taken as initial geometries for the free energy calculations. Calculated ΔG_{solv} values heavily depend on the initial conformation taken into consideration. To tackle this problem we have undertaken the following

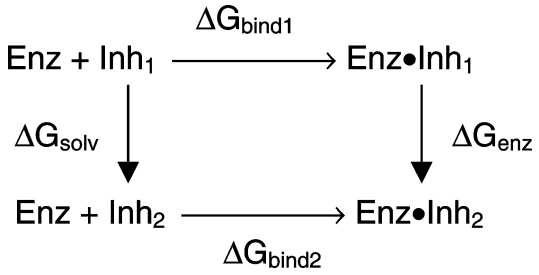

FIGURE 3 Thermodynamic cycle used for free energy calculations.

approach. We generated two, 5 nsec each, molecular dynamics trajectories of the JG-365 inhibitor in aqueous solution, initiated from two different conformations, which will be called "native" and "extended" trajectories. The "native" trajectory was initiated from the conformation found in the crystal structure of the enzyme-inhibitor complex, while the "extended" trajectory began from the beta-type conformation. Approximately 900 TIP3P [14] water molecules have been used to solvate inhibitor and a periodic boundary condition, as well as 8 A cutoff has been applied in each case. All calculations presented here have been carried out using AMBER program [15] with its force field [16]. Solute coordinates have been saved during molecular dynamics simulation after each 0.02 psec of time evolution and for each trajectory the 250,000 configurations have been collected. Generated in this way trajectories were then analyzed using neural network clustering method [2, 17], which facilitated finding the most representative conformational states of the inhibitor in aqueous solution in those trajectories.

The neural network analysis applied here was a modification of the method proposed by Karpen *et al.* [17]. The most important difference is such that presented here analysis has been carried out in dihedral space instead of Cartesian space, and cosine was used as a metric instead of Cartesian metric [3]. The JG-365 inhibitor has the 25 most important dihedral angles, thus each conformation state can be represented as a 25-dimensional vector in dihedral space. During clustering analysis we decided to take into further consideration only those clusters, which contain more than 3000 members. Other, less numerous were discarded as less important. The conformations closest to the centers of those largest, the most populated clusters have been used as starting points in the free energy perturbation (FEP) molecular dynamics simulations. Such an approach allowed us to pinpoint the most important features of the conformational transition of the solute in aqueous solution and to gain insight on how the simulated free energies depend on the initial conformation. Unfortunately, there is no guarantee that conformations found here for normal inhibitor could be also representative for the peptidomimetic inhibitors. The similar neural network clustering analysis should be performed for the mutated molecules as well. Finding then appropriate paths in the conformational space connecting normal and fully perturbed states during molecular dynamics – free energy perturbation simulations would be quite a challenging task and has not been undertaken here.

As a result of our clustering analysis for the normal inhibitor we have been able to find seven and nine of the most populated clusters in the "native" and "extended" trajectory, respectively. The generated trajectories

can be characterized in terms of transitions between those clusters. There are many ways to present results of clustering analysis, but we think that the most interesting one is, for example, the cluster-to-cluster connectivity presented in the Table I, and the rms deviations between geometries of various conformers closest to the centers of largest clusters (Tab. II).

TABLE I Cluster-to-cluster connectivity of the clusters obtained from the JG-365 molecular dynamics in aqueous solution trajectory analysis

	*n*1	*n*2	*n*3	*n*4	*n*5	*n*6	*n*7
Native trajectory							
n1	5746	1	18	1	0	0	0
n2	1	3415	0	0	0	0	0
n3	18	0	20412	0	0	0	0
n4	0	0	0	6952	1	0	0
n5	0	0	0	0	11505	1	0
n6	0	0	0	0	0	6381	1
n7	0	0	0	0	0	0	6541
Extended trajectory							
	*e*1	*e*2	*e*3	*e*4	*e*5	*e*6	*e*7	*e*8	*e*9
e1	7165	1	0	0	0	0	0	0	0
e2	0	6799	1	0	0	0	0	0	0
e3	0	0	8991	1	0	0	0	0	0
e4	0	0	0	6546	1	0	0	0	0
e5	0	0	0	0	8978	1	0	0	0
e6	0	0	0	0	0	6435	463	2	2
e7	0	0	0	0	0	462	7202	3	0
e8	0	0	0	0	0	1	2	6743	397
e9	0	0	0	0	0	3	0	396	5805

TABLE II Rms deviations (in A) between native and extended conformations closest to the centers of appropriate clusters. Only heavy atoms are taken into account

	*n*2	*n*3	*n*4	*n*5	*n*6	*n*7	*e*1	*e*2	*e*3	*e*4	*e*5	*e*6	*e*7	*e*8	*e*9
n1	2.1	1.0	2.2	2.6	3.2	2.7	3.5	4.2	4.0	4.1	2.8	2.5	2.7	2.6	3.1
n2	–	1.9	3.1	3.2	4.0	3.1	3.7	4.4	4.4	4.4	3.5	3.4	3.4	3.3	3.8
n3		–	2.4	2.6	3.2	2.6	3.7	4.5	4.3	4.4	2.8	2.6	2.7	2.6	3.1
n4			–	1.4	3.0	2.9	3.4	4.2	3.8	3.9	2.6	2.6	2.6	2.8	3.0
n5				–	2.8	2.5	3.9	4.4	4.2	4.4	2.8	2.9	2.8	2.9	3.2
n6					–	2.2	4.3	4.1	4.1	4.3	2.3	2.0	2.3	2.3	2.2
n7						–	4.4	4.4	4.4	4.5	1.9	2.1	1.8	1.9	2.2
e1							–	2.2	2.3	2.2	4.0	4.1	4.2	4.2	4.1
e2								–	1.8	1.7	4.2	4.2	4.3	4.1	4.0
e3									–	1.2	3.9	4.1	4.1	4.1	3.9
e4										–	4.1	4.2	4.3	4.3	4.0
e5											–	1.4	0.7	1.1	1.2
e6												–	1.1	1.3	1.3
e7													–	0.8	1.1
e8														–	1.0

The cluster-to-cluster connectivity table (Tab. I) contains the following information: on diagonal the number of members belonging to a given cluster, and off-diagonal values represent the number of transitions between two clusters. This is time-independent picture, but allows for pinpointing the most important features of conformational evolution of the solute in water solution. In most cases transition between two clusters involves simultaneous change of two dihedral angles. The "native trajectory evolved mainly linearly with time, *e.g.*, a given cluster is accessed from the immediate previous one, although at the initial stage few transitions between first three clusters can be observed. The most populated cluster is the "n3" from the "native" trajectory. It is interesting to find out, that the cluster "n4" is not accessible immediately from the "n3". This transition is forbidden because of geometrical constraints. The same effect is observed in the case of last 1.3 nsec of "extended" trajectory, which is mainly represented by the "e6"-"e9" clusters. There are many frequent jumps between the "e6"-"e7", and "e8"-"e9", less frequent between the "e6"-"e9" or "e6"-"e8" but totally forbidden between the "e7"-"e9", which can also be rationalized on the basis of geometrical hindrance. Such an analysis also shows that a given cluster is not necessary always a contiguous in time evolution.

In Table II appropriate rms deviations between conformations closest to the centers of appropriate clusters are presented. Only heavy atoms are considered in the rms calculations. As one can see, at the initial stage of the molecular dynamics simulations the native and extended trajectories differ substantially, but at the end of their 5 nsec duration they became more similar to each other, *e.g.*, rms between the n6-n7 and e6-e9 conformers taken from the last portion of both trajectories fall below 2.5 A value. However, it does not mean, that the trajectories already have converged.

The representatives from both trajectories, *e.g.*, conformations closest to the centers of appropriate clusters were taken as initial geometries for the free energy perturbation calculations. The results of those simulations are summarized in the Tables III – VI. The errors of the ΔG_{enz} and ΔG_{solv}, in any case does not exceed the value of 0.5 kcal/mol. Negative values for $\Delta\Delta G_{bind}$ indicate that a given mutation may be beneficial from the binding point of view. For example, increasing binding constants could be achieved (a) by replacing the third (between LEU-ASN) and fifth (between PRO-ILE) peptide bonds with —CH═CH— unit, (b) by replacing the fourth (between LEU-ASN) and sixth (between ILE-VAL) peptide bonds with —CF═CH— unit. Also our results demonstrate which mutation should not be attempted, for example replacing the peptide bond by an ethylene unit in the P2-P1 site (between ASN-PHE, peptide bond number 4) should decrease

TABLE III The —CO—NH— → —CH=CH— perturbation in JG-365. (ASP25 protonated in the enzyme). Energies in kcal/mol

Bond no. between	ΔG_{enz}	ΔG_{solv}	$\Delta\Delta G_{bind} = \Delta G_{enz} - \Delta G_{solv}$
1 ACE-SER	4.0	−0.9	4.9 ± 0.2
2 SER-LEU (P4 – P3)	4.5	−0.5	5.0 ± 0.2
3 LEU-ASN (P3 – P2)	−0.8	1.3 (306 ps)	−2.1 ± 0.3
		min 0.2	−1.0 ± 0.5
		max 3.1	−3.9 ± 0.5
4 ASN-PHE (P2 – P1)	7.9	1.7	6.2 ± 0.3
5 PRO-ILE (P1′ – P2′)	6.9	9.7 (306 ps)	−2.8 ± 0.5
		min 6.2	0.7 ± 0.7
		max 11.4	−4.5 ± 0.2
6 ILE-VAL (P2′ – P3′)	4.2	5.5 (306 ps)	−1.3 ± 1.3
7 VAL-NME	5.8	−2.3	8.1 ± 2.1

TABLE IV The —CO—NH— → —CH=CH— perturbation in JG-365. (ASP125 protonated in the enzyme). Energies in kcal/mol

Bond no. between	ΔG_{enz}	ΔG_{solv}	$\Delta\Delta G_{bind} = \Delta G_{enz} - \Delta G_{solv}$
3 LEU-ASN (P3 – P2)	0.6	1.3 (306 ps)	−0.7 ± 0.3
		min 0.2	0.4 ± 0.5
		max 3.1	−2.5 ± 0.5
5 PRO-ILE (P1′ – P2′)	11.4	9.7 (306 ps)	1.7 ± 0.5
		min 6.2	5.2 ± 0.7
		max 11.4	0.0 ± 0.2

TABLE V The —CO—NH— → —CF=CH— perturbation in JG-365. (ASP25 protonated in the enzyme). Energies in kcal/mol

Bond no. between	ΔG_{enz}	ΔG_{solv}	$\Delta\Delta G_{bind} = \Delta G_{enz} - \Delta G_{solv}$
1 ACE-SER	3.7	3.4	0.3 ± 0.8
2 SER-LEU (P4 – P3)	4.7	1.1	3.6 ± 1.0
3 LEU-ASN (P3 – P2)	2.3	2.0 (306 ps)	0.3 ± 0.4
4 ASN-PHE (P2 – P1)	4.4	5.4	−1.0 ± 1.0
5 PRO-ILE (P1′ – P2′)	4.8	2.6 (306 ps)	2.2 ± 0.2
6 ILE-VAL (P2′ – P3′)	4.2	5.4 (306 ps)	−1.2 ± 0.4
7 VAL-NME	5.7	−0.1	5.8 ± 1.4

TABLE VI The —CO—NH— → —CF=CH— perturbation in JG-365. (ASP125 protonated in the enzyme). Energies in kcal/mol

Bond no. between	ΔG_{enz}	ΔG_{solv}	$\Delta\Delta G_{bind} = \Delta G_{enz} - \Delta G_{solv}$
1 ACE-SER	3.8	3.4	0.4 ± 0.9
2 SER-LEU (P4 – P3)	4.8	1.1	3.7 ± 1.1
3 LEU-ASN (P3 – P2)	1.8	2.0 (306 ps)	−0.2 ± 0.4
4 ASN-PHE (P2 – P1)	5.8	5.4	0.4 ± 1.0
5 PRO-ILE (P1′ – P2′)	3.6	2.6 (306 ps)	1.0 ± 0.2
6 ILE-VAL (P2′ – P3′)	7.0	5.4 (306 ps)	1.6 ± 0.9
7 VAL-NME	5.2	−0.1	5.3 ± 1.7

the inhibition effect. This result is consistent with some experimental work of Keenan *et al.* [18].

Tables III–IV demonstrate also the range of free energy values (min and max values) obtained from free energy perturbations carried out in aqueous solution when starting from different geometries, *e.g.*, from conformations that were closest to the centers of appropriate clusters. As can be seen, the simulated ΔG_{solv} values could differ from each other by more than 5.0 kcal/mol depending on the initial structure taken as a starting point. If the initial inhibitor geometry was chosen to be the one from the largest cluster ("n3"), then the calculated ΔG_{solv} values were always found to be between upper and lower values found altogether.

DRUG-DNA FREE ENERGY CALCULATIONS

Recently, a new approach, developed by Srinivasan *et al.* [19–20] has gained substantial interest. It is based on an analysis of molecular dynamics trajectories using a continuum solvent approach. In this approach the molecular dynamics simulation is carried out for the solute in aqueous solution. Then the solute trajectory is extracted from its aqueous environment, each separate snapshot of the solute is analyzed using continuum solvent methods and the average free energy over the trajectory is calculated. The electrostatic contribution to the solvation free energy is calculated using the Poisson-Boltzmann (PB) [21] or the Generalized Born (GB) formula [22]. The study of the effect of added salt on the solute can be also computed either by a linear or nonlinear solution to the PB equation with an additional salt term added [23]. The non-polar contribution to the solvation free energies is calculated by additional term that is dependent on the solvent accessible surface area (SA) [24]. The solute entropy contribution can be estimated by performing normal mode analysis. Finally, the internal energy (gas phase) for each snapshot is calculated as the molecular mechanical energy using the same force field parameters, which were applied in the molecular dynamics simulation. Thus, total free energy of the solute is calculated:

$$G_{water} = E_{gas} + G_{solvation} - TS, \tag{2}$$

where:

$$G_{solvation} = G(PB \text{ or } GB)_{elstat} + G_{non\text{-}polar} \tag{3}$$

$$E_{gas} = E_{internal} + E_{electrostatic} + E_{vdw} \quad (4)$$

$$G_{non\text{-}polar} = \gamma\ SA + b \quad (5)$$

Based on above equations the free energy of binding between two biomolecules in water solution can be calculated according to:

$$\Delta G_{binding} = G_{water}\ (complex) - G_{water}\ (monomer1) - G_{water}\ (monomer2) \quad (6)$$

Using this approach the values of the ΔG_{bind1} and ΔG_{bind2} from the cycle in Figure 3 could be calculated directly instead of simulating horizontal processes. Although, this approach gives less accurate results compared to the FEP method, it is more general and can be easily applied to large interacting systems.

We have applied the continuum post-analysis method to rationalize DNA-drug interaction complexes [25]. We chose to study the following systems: actinomycin interacting with $d(GAAGCTTC)_2$ duplex, its chromophore–phenoxazone with the same DNA fragment, the acridine intercalator with the same DNA duplex and finally netropsin with $d(CGCGAATTCGCG)_2$. The antibiotic actinomycin is an antitumor drug, which contains a planar phenoxazone ring intercalating into the DNA and two pentapeptide lactone rings binding to minor groove in a sequence specific manner. It has been shown that binding actinomycin to DNA is entropy driven [26, 27]. Phenoxazone ring system intercalates between middle GC base pairs. The acridine is an example of charged intercalator, and netropsin is another drug [27], which is characterized by very high binding free energy. Its binding is enthalpy driven and it binds specifically to AATT sequences into the minor groove. The structures of those drugs are shown in Figure 4.

DNA-drug molecular dynamics simulations have been initiated from appropriate crystallographic structures in the case of actinomycin-DNA [26] and netropsin-DNA [27] complexes, and from model built structures for the acridine-DNA complexes. The acridine-DNA complexes have been built using a crystallographic structure of the actinomycin' chromophore-DNA intercalation complex as a template. In each case the 1 nsec long molecular dynamics simulations have been performed using TIP3P water molecules [14], periodic boundary conditions, particle mesh Ewald method [29] for electrostatic energy calculations, and Cornell *et al.*, force field [30]. For continuum solvent MD trajectory post-analysis the 100 structures/snapshots have been used in order to obtain the mean values. Entropy contribution to

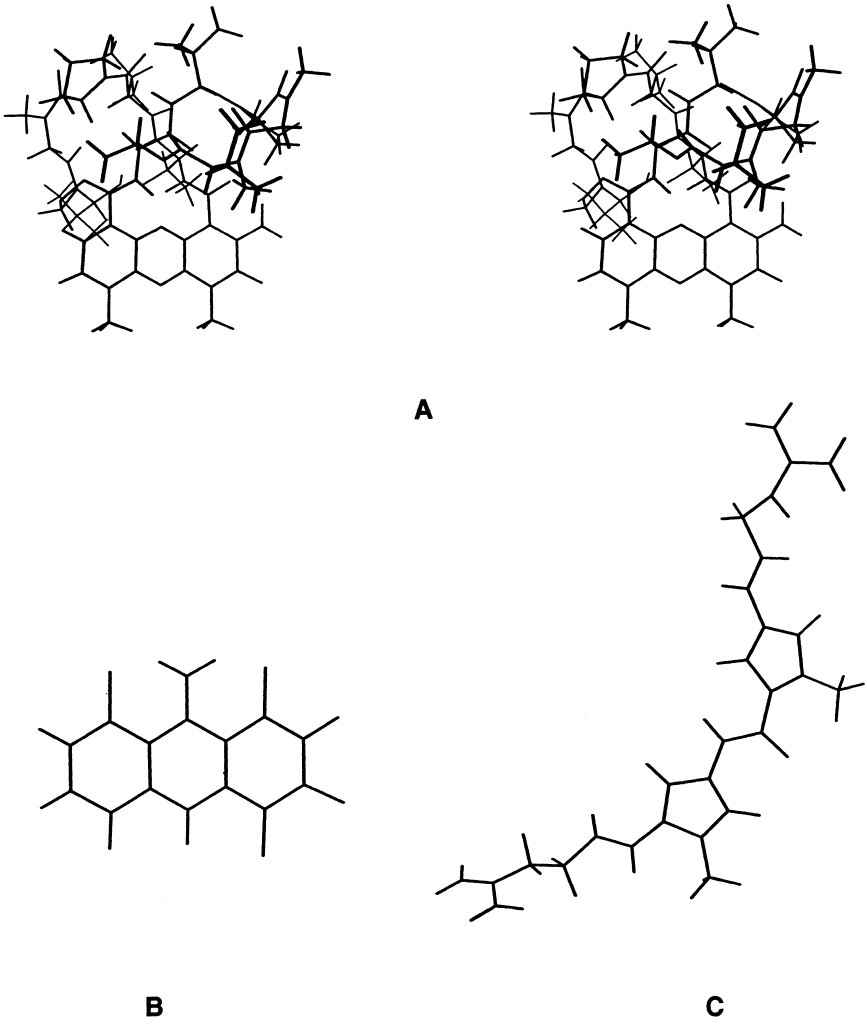

FIGURE 4 Structures of the drugs used in the case of DNA-drug complexes free energy calculations: (a) – stereoview of actinomycin, (b) – acridine, (c) – netropsin.

solvation free energies has not been included here. There are few practical methods of entropy calculation based on molecular simulations. For example, the most popular one employs the normal mode analysis [19, 20], the other one is a method of Schlitter [31], which is based on analysis of the covariance matrix. Calculation of the entropy contribution to the free energies of the DNA-drug complexes is still under investigation and will be discussed more extensively in Ref. [25].

The following information could be obtained from this type of DNA-drug simulations and continuum solvent analysis: the DNA-drug binding energies, the DNA deformation upon drug binding, the DNA intrastrand interactions and sequence-dependent unstacking free energies due to intercalation. Some of the representative calculated free energies are presented in Tables VII–IX. The energy values obtained immediately from continuum solvent trajectory post-analysis, which are subsequently used to derive DNA-deformation, binding and unstacking free energies (see Tabs. VII and IX) have the errors, which do not exceed the 15% of their absolute values. The entropy contribution as well as the role of ionic strength [23] is still under investigation and will be discussed elsewhere [25]. Those two effects, which are not included in the present results, could be partially responsible for the discrepancies between calculated and experimental DNA-drug binding free energies presented in Table VII. It is surprising to see a good agreement between calculated and experimental $\Delta G_{\text{binding}}$ for

TABLE VII DNA-deformation and DNA-drug binding energies (kcal/mol)

	$\Delta G_{DNA\text{-}deformation}$	$\Delta G_{binding}$	$\Delta G_{binding}(exp)$
Actinomycin + $(GAAG\text{-}CTTC)_2$	37.4	−10.4	−9.0
Phenoxazine + $(GAAG\text{-}CTTC)_2$	24.1	−0.5	> -4.0
Acridine + $(GAAG\text{-}CTTC)_2$	28.8	+4.7	~ -8
Acridine + $(GAAC\text{-}GTTC)_2$	24.0	−0.5	
Netropsin + $(CGCGAATTCGCG)_2$	7.5	−21.8	−11.5

TABLE VIII DNA intrastrand interaction free energies (kcal/mol)

	DNA unbound	*DNA bound*	$\Delta\Delta G$ *change upon binding*
Actinomycin + $(GAAG\text{-}CTTC)_2$	-30.9 ± 4.7	-21.3 ± 3.9	9.6
Phenoxazine + $(GAAG\text{-}CTTC)_2$	-30.9 ± 4.7	-23.5 ± 4.3	7.4
Acridine + $(GAAG\text{-}CTTC)_2$	-30.9 ± 4.7	-26.1 ± 4.5	4.8
Acridine $(GAAC\text{-}GTTC)_2$	-30.1 ± 3.6	-26.2 ± 4.0	3.9
Netropsin + $(CGCGAATTCGCG)_2$	-51.3 ± 5.6	-49.4 ± 5.4	1.9

TABLE IX Base pairs unstacking free energies (kcal/mol)

	unstacking	$\Delta G_{unstacking}$
Actinomycin-$(GAAG\text{-}CTTC)_2$	-GC-	13.9
Chromophore-$(GAAG\text{-}CTTC)_2$	-GC-	8.4
Acridine-$(GAAG\text{-}CTTC)_2$	-GC-	12.0
Acridine-$(GAAC\text{-}GTTC)_2$	-CG-	10.2

actinomycin-DNA complex, since entropy contribution was not included in reported here value, and according to experimental work this complex formation is entropy driven [26]. On the other hand, in agreement with experimental data the acridine molecule prefers to intercalate between the CG base pairs rather than the GC ones. This is related to the fact that it cost less free energy to unstuck CG sequence compared to the GC. This effect is confirmed by the results presented in Tables VIII and IX.

The DNA deformation free energies (Tab. VII), calculated as differences between bound and unbound configurations of DNA fragments, reflect the substantial role of intercalators in distorting double helices. The largest deformation is observed in the case of actinomycin, where minor groove binding process is accompanied by intercalation of phenoxazone rings, the smallest deformation is due to netropsin, which binds perfectly into the minor groove. Table VIII contains DNA intrastrand interaction free energies for bound and unbound forms. The results demonstrate once again that it is easier to unstuck the C-G sequences compared to the G-C, in the case of intercalation complexes, as well as that the DNA intrastrand interaction is only slightly affected by minor groove binder – the netropsin molecule.

CONCLUSION

We presented here the results from application of two methods devised to calculate free energies based on molecular dynamics simulations. Each of them applies to different paths of the thermodynamics cycle presented in Figure 3. It seems that free energy perturbation is well suited to small perturbations within the molecular systems, while continuum solvent approaches, although still less accurate, can be applied to more complex and larger systems. It would be of interest to apply both of those methods to the same system to calculate all paths in the thermodynamics cycle in order to check for its closure and to assess the quality of the continuum solvent methods. Such an approach could be potentially used to improve the continuum method, which has been applied in this study.

Acknowledgment

This work is partially supported by Polish KBN Grant no. 3T09A 096 19 and FIRCA/NIH 1 R03-TW01234-01.

References

[1] Cieplak, P. and Kollman, P. A. (1993). Peptide mimetics as enzyme inhibitors: Use of free energy perturbation calculations to evaluate isosteric replacement for amide bonds in a potent HIV protease inhibitor, *J. Comp. - Aided Mol. Design*, **7**, 291–304.

[2] Cieplak, P., Kollman, P. A. and Radomski, J. P. (1996). Molecular design of fluorine-containing peptide mimetics, Chapt.11, pp. 143–156, *ACS Symposium Series* v. **639**, 1996. Biomedical Frontiers of Fluorine Chemistry, Eds. Ojima, I., McCarthy, J. R. and Welch, J. T., ACS Books, *American Chemical Society* Washington, D.C.

[3] Cieplak, P. and Radomski, J. P. (2001). "*Conformational States of the HIV aspartic protease inhibitor JG-365 in aqueous solution. Clustering and free energy perturbation analysis*", in preparation.

[4] Johnston, M. I. and Hoth, D. F. (1993). Present and future prospect for HIV therapies, *Science*, **260**, 1286–1293.

[5] Roberts, N. A., Martin, J. A., Kinchington, D., Broadhurst, A. V., Craig, J. C., Duncan, I. B., Galpin, S. A., Handa, B. K., Kay, J., Krohn, A., Lambert, R. W., Merrett, J. H., Mills, J. S., Parkes, K. E. B., Redshaw, S., Ritchie, A. J., Taylor, D. L., Thomas, G. J. and Machin, P. J. (1990). Rational drug design of peptide based HIV proteins inhibitors, *Science*, **248**, 358–361.

[6] Wlodawer, A. and Vondrasek, J. (1998). Inhibitor of HIV-1 protease: A major success of structure-assisted drug design, *Ann. Rev. of Biophysics and Biomolecular Structure*, **27**, 249–284.

[7] Goldgur, Y., Craigie, R., Cohen, G. H., Fujiwara, T. *et al.* (1999). Structure of the HIV-1 integrase catalytic domain complexed with an inhibitor: A platform for antivirial drug design, *Proc. of the Nat. Acad. of Sciences*, US, **96**, 13040–13043.

[8] Cox, M. T., Gormley, J. J., Hayward, C. F. and Petter, N. N. (1980). Incorporating of trans-olefinic dipeptide isosters into enkephalin and substance P analogs, *J. of Chemical Society-Chemical Communications*, **17**, 800–802.

[9] Hann, M. M., Sammes, P. G., Kennewell, P. D. and Taylor, J. B. (1980). Double bond isosteres of the peptide bond enkephalin analog, *J. of Chemical Society-Chemical Communications*, **5**, 234–235.

[10] Bash, P. A., Singh, U. C., Langridge, R. and Kollman, P. A. (1987). Free energy calculation by computer simulations, *Science*, **236**, 564–568.

[11] Beveridge, D. L. and DiCapua, F. M. (1989). Free energy *via* molecular simulation: A primer, in Computer Simulation of Biomolecular Systems, *Theoretical and Experimental Applications*, Eds.: van Gunsteren, W. F. and Weiner, P. K., pp. 1–26, ESCOM, The Netherlands.

[12] Swain, A. L., Miller, M. M., Green, J., Rich, D. H., Schneider, J., Kent, S. B. H. and Wlodawer, A. (1990). X-ray crystallographic structure of a complex between a synthetic protease of human immunodeficiency virus-1 and a substrate-based hydroxyethylamine inhibitor, *Proc. Natl. Acad. Sci.* U.S.A., **87**, 8805–8809.

[13] Miller, M. M., Schneider, J., Sathyanarayanam, B. K., Toth, M. V., Marshall, G. R., Clawson, L., Selk, L., Kent, S. B. H. and Wlodawer, A. (1989). Structure of complex of synthetic HIV-1 protease with a substrate-based inhibitor at 2.3A resolution, *Science*, **246**, 1149–1152.

[14] Jorgensen, W., Chandrasekhar, J., Madura, J., Impey, R. and Klein, M. (1983). Comparison of simple potential functions for simulating liquid water, *J. Chem. Phys.*, **79**, 926–935.

[15] AMBER version 4.0 (1991). Pearlman, D. A., Case, D. A., Caldwell, J., Seibel, G. L., Singh, U. C., Weiner, P. and Kollman, P. A., Department of Pharmaceutical Chemistry, University of California, San Francisco.

[16] Weiner, S. J., Kollman, P. A., Nguyen, D. T. and Case, D. (1986). An all atom force field for simulations of proteins and nucleic acids, *J. Comput. Chem.*, **7**, 230–252.

[17] Karpen, M. E., Tobias, D. J. and Brooks III, Ch. L. (1993). Statistical clustering techniques for the analysis of long molecular dynamics trajectories – analysis of 2.2 ns trajectories of YPGDV, *Biochemistry*, **32**, 412–420.

[18] Keenan, R. M., Eppley, D. F. and Tomaszek, Th. A. Jr. (1995). Synthesis and activity of an HIV-1 protease inhibitor containing a contiguous (E)-olefin-hydroxyethylene peptide mimetic, *Tetrahedron Lett*., **36**, 819–822.
[19] Cheatham III, T. E., Srinivasan, J., Case, D. A. and Kollman, P. A. (1998). Molecular dynamics and continuum solvent studies of the stability of polyG-polyC and polyA-polyT DN duplexes in solution, *J. Biomol. Struct. and Dynamics*, **16**, 265–280.
[20] Srinivasan, J., Cheatham III, T. E., Cieplak, P., Kollman, P. A. and Case, D. A. (1998). Continuum solvent studies on the stability of DNA, RNA and phosphoramidate–DNA helices, *J. Amer. Chem. Soc*., **120**, 9401–9409.
[21] Honig, B., Sharp, K. A. and Yang, A.-S. (1993). Macroscopic models of aqueous solutions – biological and chemical applications, *J. Phys. Chem*., **97**, 1101–1109.
[22] Still, W. C., Tempczyk, A., Hawley, R. C. and Hendrickson, T. (1990). Semianalytical treatment of solvation for molecular mechanics and dynamics, *J. Amer. Chem. Soc*., **112**, 6127–6129.
[23] Sharp, K. A. and Honig, B. (1995). Salt effects on nucleic acids, *Current Opinion in Struct. Biology*, **5**, 323–328.
[24] Sitkoff, D., Sharp, K. A. and Honig, B. (1994). Accurate calculation of hydration free energies using macroscopic solvent models, *J. Phys. Chem*., **98**, 1978–1988.
[25] Cieplak, P. and Kollman, P. A. (2001). Drug-DNA free energy calculations, in preparation.
[26] Berman, H. M., Ginell, S. L., Sawzik, P. and Lessinger, L. (1988). Structural characteristic of Actinomycin D that form the basis for its interactions with DNA, *Structure and Expression*, Vol. 2: DNA and Its Drug Complexes, Eds. Sarma, R. H. and Sarma, M. H., Adenine Press, 1988, pp. 317–328.
[27] Marky, L. A., Snyder, J. G., Remeta, D. P. and Breslauer, K. J. (1983). Thermodynamics of drug-DNA interactions, *J. of Biomol. Structure and Dynamics*, **1**, 487–513.
[28] Muller, W. and Crothers, D. M. (1968). Studies of the binding of actinomycin and related compounds to DNA, *J. Mol. Biol*., **35**, 251–290.
[29] Essmann, U., Perera, L., Berkowitz, M. L., Darden, T., Lee, H. and Pedersen, L. G. (1995). A smooth particle mesh Ewald method, *J. Chem. Phys*., **103**, 8577–8593.
[30] Cornell, W. D., Cieplak, P., Bayly, C. I., Gould, I. R., Merz, K. M., Ferguson, D. M., Spellmeyer, D. C., Fox, T., Caldwell, J. W. and Kollman, P. A. (1995). A Second Generation Force Field for Simulation Proteins, Nucleic Acids and Related Organic Molecules. *J. Am. Chem. Soc*., **117**, 5179–5197.
[31] Schlitter, J. (1993). Estimation of absolute and relative entropies of macromolecules using the covariance matrix, *Chem. Phys. Lett*., **215**, 617–621.